ACS chemical biology

Article

Imaging of Tie2 with a fluorescently labeled small molecule affinity ligand

Peter David Koch, Maaz S. Ahmed, Rainer H. Kohler, Ran Li, and Ralph Weissleder

ACS Chem. Biol., **Just Accepted Manuscript** • DOI: 10.1021/acschembio.9b00724 • Publication Date (Web): 06 Dec 2019

is published by the American Chemical Society. 1155 Sixteenth Street N.W., Washington, DC 20036

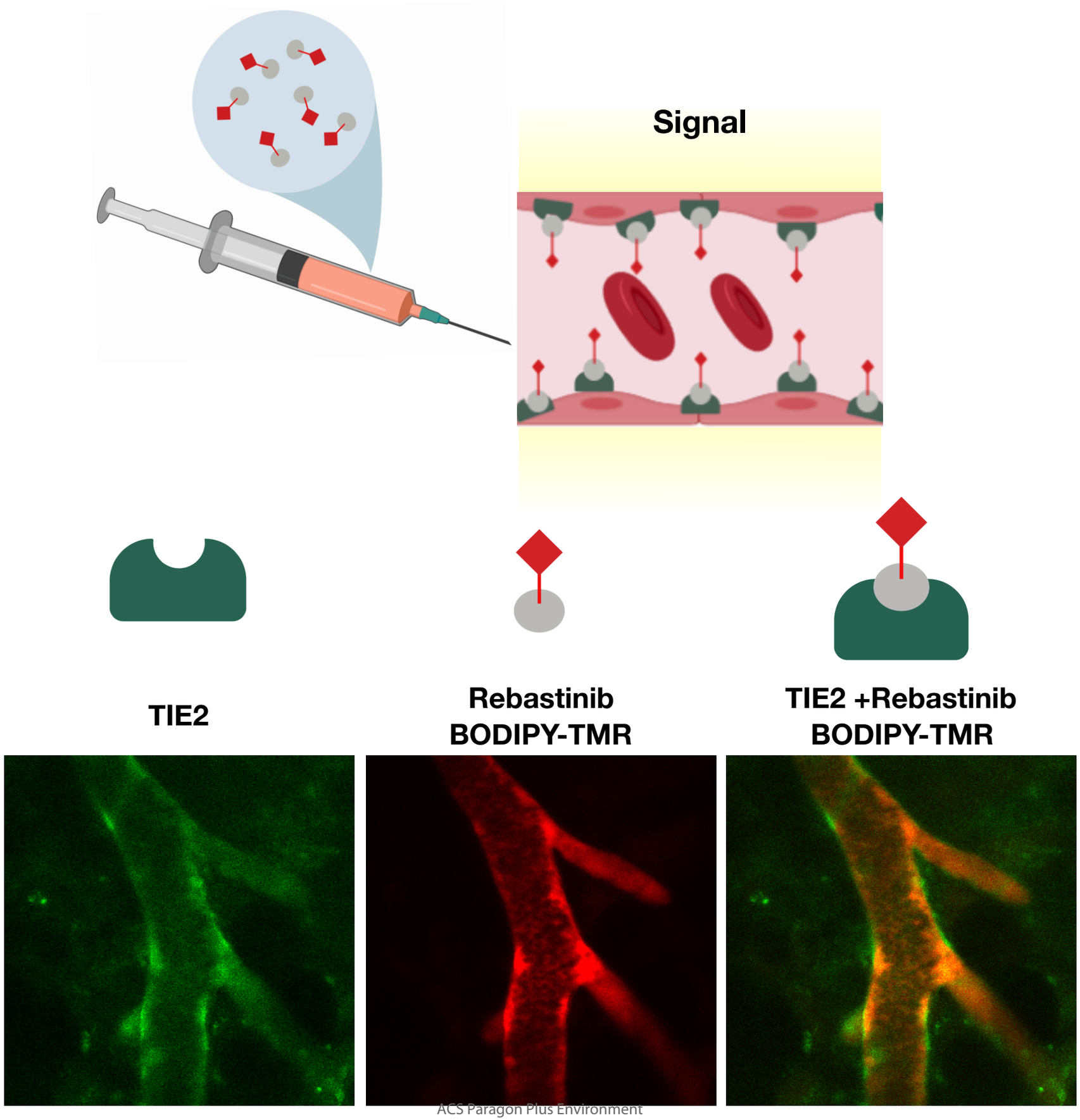
Signal
TIE2
Rebastinib
BODIPY-TMR
TIE2 +Rebastinib
BODIPY-TMR

Imaging of Tie2 with a fluorescently labeled small molecule affinity ligand

Peter David Koch[1,3], Maaz S. Ahmed[1,3], Rainer H. Kohler[1], Ran Li[1], Ralph Weissleder[1,2,4]
1.Center for Systems Biology, Massachusetts General Hospital, Boston, MA 02115
2.Department of Systems Biology, Harvard Medical School, Boston, MA 02115
3.These authors contributed equally
4.Correspondence: rweissleder@mgh.harvard.edu

Abstract

The receptor tyrosine kinase inhibitor, Tie2, has significant roles in endothelial signaling and angiogenesis, and is relevant in the pathophysiology of several diseases. However, there are relatively few small molecule probes available to study Tie2, making evaluation of its activity *in vivo* difficult. Recently, it was discovered that the small molecule, rebastinib (DCC-2036), is a potent Tie2 inhibitor. We hypothesized that fluorescent derivatives of rebastinib could be used as imaging agents for Tie2. Based on crystallography structures, we synthesized three fluorescent derivatives, which we then evaluated in both *in vitro* and *in vivo* assays. We found that the Rebastinib-BODIPY TMR (Reb-TMR) derivative has superior imaging characteristics *in vitro*, and successfully labeled endothelial cells *in vivo*. We propose that this probe could be further used in *in vivo* applications for studying the role of Tie2 in disease.

Introduction

The angiopoietin-Tie2 signaling pathway plays an important role in regulating vascularization and angiogenesis. Angiopoietins comprise a set of 4 growth factors, Ang1 through Ang4, which bind to Tie2, a receptor tyrosine kinase that activates downstream signaling pathways[1,2]. Tie2 is closely related to the receptor Tie1, and sometimes functions as a heterodimer. Both are predominately expressed in endothelial cells. Binding of Tie2 to its agonist ligand, Ang1, activates the receptor and promotes angiogenesis via several pathways and downstream nodes, such as Akt, FOXO, and NFkB[1,2]. Other angiopoietins, such as Ang2, also bind to Tie2 and can promote angiogenesis; however, the effects induced by other angiopoietins are context dependent and in fact can sometimes inhibit angiogenesis.

Dysregulation of the Ang-Tie2 pathway has been linked to several diseases. For example, it has been observed that Tie2 levels are reduced in model systems of neovascular age-related macular degeneration (NV-AMD), a condition characterized by irregular, leaky vasculature in the choriod that leads to progressive vision loss[3]. It has been shown that activation of the Tie2 pathway with an agonistic antibody is effective in mouse models of NV-AMD, improving vascularization without the side effects associated with current standard of care anti-VEGF therapy. Relatedly, activation of the Tie2 receptor with the same agonistic antibody also has proven beneficial in mouse models of sepsis, as it normalized the vasculature[4]

Overactivation of the Ang-Tie2 pathway, on the other hand, is typically pro-tumorigenic[5,6,7]. Hypoxic conditions can trigger production of Tie2, which stimulates tumorigenesis through a number of pro-wound healing mechanisms[8,9,10]. Curiously, it has been observed that Tie2 is also expressed in macrophages, and the presence of Tie2-positive macrophages in biopsies is associated with higher risks of metastasis[5,6]. Conversely, there are some studies suggesting that activation of the Tie2 pathway with a phosphatase inhibitor can enhance immunotherapy[11], but to date, most work suggests that this pathway promotes tumorigenesis. Indeed, it is increasingly clear that the tumor microenvironment, including both stromal and immune cells, plays a substantial role in therapy. Further study in the role of Tie2 in cancer tumor microenvironment is warranted.

Despite the various roles of Tie2 in disease pathophysiology, it is still comparatively less studied, especially *in vivo*. One challenging factor is that there are limited small molecule probes available to study its activity. Recently however, it was discovered that rebastinib, a kinase inhibitor in clinical trials for refractory leukemia, exhibits potent activity against Tie2. Rebastinib is a small molecule drug that functions as a switch control inhibitor; it binds at an allosteric site and induces the kinase to adopt inactive conformation[12]. Given the emerging roles of Tie2 in disease, and the need for more probes to study Tie2, we developed companion imaging agents based off a rebastinib scaffold to study Tie2 in various model systems. Specifically, we synthesized three derivatives, evaluated their activities in *in vitro* cell culture assays, and finally tested the utility of one lead compound in an *in vivo* setting.

Methods

Synthesis of fluorescent derivatives

For description of the synthesis of the fluorescent rebastinib analogs, please refer to the supplementary material.

Cell culture, in vitro assays, and immunofluorescence

HUVEC cells were maintained in Lonza Endothelial Growth Medium-2 (EGM™-2) with supplements added as per manufacturer instructions (Lonza, CC-3162). HEK293T and RAW264.7 cells were maintained in Dulbecco's Modified Eagle Medium (DMEM) supplemented with 10% fetal bovine serum (Atlanta Biologicals) and 1% penicillin-streptomycin (Thermo Fisher). Cells were incubated at 37°C, 5% CO2.

TIE2 plasmid was obtained from SinoBiological (HG10700-NY). For transfection of Tie2 plasmid, the Fugene 6 transfection kit (Promega, E2691) was used, following protocol of manufacturer.

For microscopy assays, Corning 3764 384-well plates were seeded with approximately 1,000 cells/well in 40 µL of media. Cells were treated with fluorescent drug and/or unlabeled drug, for 90 minutes of treatment. Wells were then washed out 6 times with 80 uL of media. Washes were performed repetitively, with no wait times. Cells were then incubated with 10 µg/mL Hoechst 333412 for 5 minutes, and then washed out, three times with 80 uL of media. Cells were subsequently imaged on either an Operetta High Content Screening System, or an IXM MetaExpress. In both cases, cells were imaged in either the 560 nm channel (BODIPY-TMR) or 650 nm channel (SiR and BODIPY-650), as well as a 360 nm channel (Hoechst 333412) to determine nuclei. Channel information for microscopy is summarized in supplementary table 1.

For co-localization assays, cells were imaged on an upright BX63 microscope (Olympus) or a Olympus high-throughput imaging system in the same channels as above with either 100x (HUVEC) or 60x (RAW264.7) magnification. Cells were treated with fluorescent drug as above and imaged after washing out drug. Cells were then fixed with 4% PFA for 20 min, blocked with 3% BSA in PBS, and then stained with a Tie2 antibody (Abcam, ab24859 for anti-mouse Tie2 and ab221154 for anti-human Tie2) at 10 µg/mL for 1 hour at room temperature. Cells were then stained with a secondary anti-mouse or anti-rabbit Alexa 647 antibody (anti-rabbit or anti-mouse Alexa 647 antibody) at 10 µg/mL and Hoechst 33342 (10 µg/mL) for 30 min.

Image analysis used in figures 3-4 was performed using the Columbus server at Laboratory of Systems Pharmacology (Harvard Medical School). In brief, nuclei were first identified using the Hoechst stain, and surrounding cellular regions were identified with the fluorescent drug. Image intensities were then quantified. Co-localization plot in figure 5 was done in ImageJ FIJI (NIH), using the Coloc2 plugin. For figure 6, blood half-life measurement was determined by quantifying fluorescent intensity in a segmented vessel area, using Cell Profiler.

For fluorescent polarization binding assay, recombinant Tie2 (Thermo Fisher, PV3628) was diluted in PBS to 0.8 uM and mixed with 0.8 uM of Reb-TMR. Tie2 was pre-incubated with unlabeled rebastinib at indicated concentrations. Assays were performed in Corning 4581 low volume, 384 well plates.

All plots presented were made in GraphPad Prism 8.

Intravital imaging

Images were acquired on a modified multiphoton/confocal FV1000 imaging system (Olympus, America) [13]. The 490 nm channel was used to image Tie2-GFP and the 560 nm channel was used to image Reb-TMR. Examination was performed in dorsal skin-fold window chambers implanted in STOCK Tg(TIE2GFP)287Sato/J reporter mice (The Jackson Laboratory). Two million mouse mammary tumor cells were suspended in 20 µl PBS and injected into the dorsal skin-fold chamber 3 days prior to treatment. Tie2 expression was examined at baseline immediately before treatment. Images were pseudo-colored and processed in FIJI (ImageJ, NIH) by adjusting brightness/contrast.

Results

Modeling and synthesis of rebastinib derivatives

We synthesized three derivatives using either BODIPY-TMR, BODIPY-650, or silicon rhodamine (SiR) as the fluorochrome. Our choice of these fluorochromes was motivated in large part by their superior performance for in vivo applications[14–18]. Synthesis of the derivatives are described in the methods (fig. 1). Ultimately, we synthesized 3 derivatives: Rebastinib-BODIPY TMR (Reb-TMR), Rebastinib-BODIPY 650 (Reb-650), and Rebastinib-SiR (Reb-SiR). Yields were highest for the BODIPY analogs, while the SiR analog had a slightly lower yield.

Synthesis was guided by molecular modeling of a previously determined crystal structure of rebastinib and Tie2[6]. Rebastinib binds to the switch control portion of Tie2. The t-butyl, urea, and fluorophenyl moieties of rebastinib make interactions with several residues in the switch control region, which promote the protein to adopt an inactive conformation, thereby inhibiting its activity. The rebastinib-Tie2 complex is very stable with a half-life of approximately 10 hours. The crystal structure showed that the terminal amide of rebastinib extends out of the binding pocket. Thus, we decided to couple fluorophores to this part of the molecule to minimize interference with the binding motif (fig. 2).

In vitro assays for validation of fluorescent rebastinib

To characterize biochemical activity of the fluorescent derivatives, we first treated HUVEC and HEK293T cells with the three derivatives at various concentrations and measured cellular uptake. These two cell lines are Tie2+ and Tie2- respectively[19, 20]. We found that both Reb-TMR and Reb-650 stained HUVEC cells brightly at low concentrations (100 nM), and expectedly showed minimal staining in the Tie2- HEK293T line (fig. 3). The Reb-SiR analog on the other hand, showed weak staining in HUVEC cells even at doses up to 1µM (fig. 3). This drug also showed high amounts of background fluorescence, even after thorough washout. These results indicated that the SiR probe is not suitable for labeling of Tie2. We did not study in depth why the Reb-SiR failed to stain well. It is has previously been shown that the fluorescence of SiR probes are sensitive to the cellular environment, which may be one possibility[21]. Other possibilities include that the Reb-SiR probe may have a high k_{off} rate and is washed out quickly or that there is plate binding. The fact that the BODIPY analogs stained HUVEC and HEK293T cells to different degrees suggests that the drugs bind to protein targets in the cells, not to internal cellular membranes nonspecifically. Between the Reb-TMR and Reb-650 analogs, the Reb-TMR showed stronger

differential staining between HUVECs and HEK293T, so we focused on this compound for all future experiments. Neither drug showed significant cytotoxicity that would prohibit its use in *in vivo* applications (fig. S1). Absorption and emission spectra are shown in fig. S2.

Characterization of Rebastinib-BODIPY TMR (Reb-TMR)

To further characterized Reb-TMR we performed a competition assay with Reb-TMR and unlabeled rebastinib (fig. 4a, b). In cell culture, we treated cells with a combination of unlabeled rebastinib and Reb-TMR; we observed that unlabeled rebastinib competes out the fluorescent signal of Reb-TMR (IC50 = 2.69 μM), indicating that Reb-TMR shares the targets of rebastinib. Moreover, comparison of Reb-TMR and BODIPY-TMR treatment showed that the free dye was taken up in negligible amounts compared to Reb-TMR (fig. S3), further confirming specific activity of the drug. Next, we also performed a complementary experiment in which we transfected HEK293T cells with a plasmid encoding for Tie2 and treated these cells with Reb-TMR. We show that fluorescent intensity levels in Tie2-transfected cells, were above that of untransfected cells, and comparable to the levels of HUVEC cells (fig. S4). In all, these cell-based assays suggest Reb-TMR binds Tie2.

We also performed a biochemical assay to measure binding to Tie2 directly. Using fluorescent polarization as an indicator of binding, we showed that Reb-TMR with Tie2 had higher anisotropy as compared to free Reb-TMR, indicating binding (fig. 4c). Additionally, pre-incubation of recombinant Tie2 with unlabeled rebastinib (10 μM) reduced the anisotropy to levels comparable to that of the free drug, suggesting that Reb-TMR can be competed out by unlabeled drug. We noted that fluorescent intensities of Reb-TMR in vitro changed upon addition of recombinant Tie2; fluorescent was enhanced about 3-fold when adding Reb-TMR to recombinant Tie2 compared to Reb-TMR in PBS (fig. S5). However, in the presence of non-fluorescent rebastinib, these levels returned to baseline.

We next treated cells with Reb-TMR and obtained higher resolution images to investigate the degree of co-localization of Reb-TMR and Tie2. In HUVEC cells, both Reb-TMR and Tie2 display a largely cytoplasmic stain, consistent with previous knowledge of biology (fig. 5). Higher signal was observed in the perinuclear region. Correlation was not perfect (r^2 = 0.88), which likely could arise due to several factors, including non-covalent binding of Reb-TMR, off-target binding/polypharmacology or delays (Koff) in subsequent immunostaining. Given that Tie2 is also expressed in macrophages, we performed the same experiment in RAW264.7 murine macrophages. There, we observed the same cytoplasmic staining of both Reb-TMR and Tie2 (fig. S6).

Use of Reb-TMR *in vivo*

To determine the suitability of Reb-TMR as an *in vivo* imaging agent, we treated Tie2-GFP mice [22]with Reb-TMR (20 mg/kg, I.V.). This mouse model expresses GFP in endothelial cells, under the control of the Tie2 promoter; higher levels of GFP correlate with more production of Tie2. Tie2-GFP reporter mice were implanted with a dorsal skin chamber and injected with mouse mammary tumor virus cells (MMTV) to both induce a wound and to stimulate tumorigenesis. Three days after injection, we confirmed development of vasculature in the window chamber, and proceeded to image various sites. As expected, strong GFP signals could be observed lining the edges of blood vessels, consistent with the location of endothelial cells. Injection of Reb-TMR into the tail vein led to rapid, strong increase in signal in the 560 nm fluorescence channel. After the free drug began to clear out of the vessel, we observed lining of Reb-TMR along the edges of the vessel, co-localizing with the Tie2+ endothelial cells (fig. 6a). To study pharmacokinetics, we performed time lapse imaging on a single blood vessel and measured fluorescent intensity throughout the whole vessel over the course of approximately three hours. Blood PK half-life

measured in a single vessel was approximately 30 min (fig. S7). The long half-life of Reb-TMR, combined with the very strong signal of Reb-TMR along the lining of blood vessels, indicates successful *in vivo* labeling of Tie2 and is promising for the utility of this probe as an *in vivo* imaging agent.

Discussions

Tie2 plays a role in a number of disease, and much study is still warranted to determine its potential as a biomarker, prognostic, and/or therapeutic target. Tie2 is predominantly expressed in endothelial cells and to a lesser extent in immune cells. While Tie2 does not necessarily directly cause pathogenesis of a disease, modulation with a drug could be a useful therapeutic strategy. Being able to determine levels and activation states of Tie2 with companion imaging agents would therefore be useful in both experimental animal models and potentially even in clinical setting.

In comparison to other receptor tyrosine kinases, Tie2 is not as thoroughly studied, and there are limited small molecule probes available. Rebastinib was only discovered activity against Tie2 relatively recently, and as such, we decided to develop small molecule imaging agents using rebastinib as a backbone. Small molecule imaging agents have proven very successful in many other example cases, such as BTK, MERTK, and B-Raf[14,23,18]. Efficacious small molecule imaging agents can be used in any mouse model, do not exhibit permanent effects, and minimize the need for costly and timely genetically engineered mouse models.

We found that the BODIPY analogs of rebastinib, in particular Reb-TMR, labeled cells *in vitro*, very brightly and potently. Our analog also proved efficacious in a reporter mouse model, suggesting its utility for use in a broader array of model systems. While we focused on Reb-TMR in this work, we found that the Reb-650 analog also showed activity (fig. 3, fig. S8), and optimization of this molecule may be warranted if a imaging agent in the 650 nm channel is needed. Ultimately, we envision the development of a small molecule agents, including radioactive probes, that could be translated into clinical use, for measurement of Tie2 levels. Activation of Tie2 is a potential therapeutic strategy for sepsis and NV-AMD, so an imaging agent to detect for presence of Tie2 could aid rapid decision making for treatment choice. Alternatively, another possibility is to encapsulate an imaging agent in a nanoparticle to selectively deliver it to macrophages. This could allow one to image specifically for the presence of Tie2+ macrophages, which is an important prognostic marker in cancer. Given that our work so far indicates that Tie2 can be imaged with a small molecule, we hope that further work can optimize companion agents further for even more efficacious activity.

Supporting Information

Toxicity data, photophysical data, biochemical data, pharmacokinetics data, chemical synthesis protocols, NMR data, HPLC purity analysis. This material is available free of charge via the internet at http://pubs.acs.org.

Acknowledgments

We thank the Laboratory of Systems Pharmacology (Harvard Medical School) for the use of the high content imaging microscopes, C. Yapp for technical assistance with imaging, and O. R. Weissleder for help with chemical purification and NMR.

References

1. Jeltsch, M., Leppänen, V. M., Saharinen, P. & Alitalo, K. (2013) Receptor tyrosine kinase-mediated angiogenesis. *Cold Spring Harb Perspect Biol 5*, 1-22
2. Leligdowicz, A., Richard-Greenblatt, M., Wright, J., Crowley, V. M. & Kain, K. C. (2018) Endothelial Activation: The Ang/Tie Axis in Sepsis. *Front Immunol 9*, 838
3. Kim, J., Park, J. R., Choi, J., Park, I., Hwang, Y., Bae, H., Kim, Y., Choi, W., Yang, J. M., Han, S., Chung, T. Y., Kim, P., Kubota, Y., Augustin, H. G., Oh, W. Y. & Koh, G. Y. (2019) Tie2 activation promotes choriocapillary regeneration for alleviating neovascular age-related macular degeneration. *Sci Adv 5*, 6732
4. Han, S., Lee, S. J., Kim, K. E., Lee, H. S., Oh, N., Park, I., Ko, E., Oh, S. J., Lee, Y. S., Kim, D., Lee, S., Lee, D. H., Lee, K. H., Chae, S. Y., Lee, J. H., Kim, S. J., Kim, H. C., Kim, S., Kim, S. H., Kim, C., Nakaoka, Y., He, Y., Augustin, H. G., Hu, J., Song, P. H., Kim, Y. I., Kim, P., Kim, I. & Koh, G. Y. (2016) Amelioration of sepsis by TIE2 activation-induced vascular protection. *Sci Transl Med 8*, 1-11.
5. Chen, L., Li, J., Wang, F., Dai, C., Wu, F., Liu, X., Li, T., Glauben, R., Zhang, Y., Nie, G., He, Y. & Qin, Z. (2016) Tie2 Expression on Macrophages Is Required for Blood Vessel Reconstruction and Tumor Relapse after Chemotherapy. *Cancer Res 76*, 6828-6838
6. Harney, A. S., Karagiannis, G. S., Pignatelli, J., Smith, B. D., Kadioglu, E., Wise, S. C., Hood, M. M., Kaufman, M. D., Leary, C. B., Lu, W. P., Al-Ani, G., Chen, X., Entenberg, D., Oktay, M. H., Wang, Y., Chun, L., De Palma, M., Jones, J. G., Flynn, D. L. & Condeelis, J. S. (2017) The Selective Tie2 Inhibitor Rebastinib Blocks Recruitment and Function of Tie2^{Hi} Macrophages in Breast Cancer and Pancreatic Neuroendocrine Tumors. *Mol Cancer Ther 16*, 2486-2501
7. Karagiannis, G. S., Pastoriza, J. M., Borriello, L., Jafari, R., Coste, A., Condeelis, J. S., Oktay, M. H. & Entenberg, D. (2019) Assessing Tumor Microenvironment of Metastasis Doorway-Mediated Vascular Permeability Associated with Cancer Cell Dissemination using Intravital Imaging and Fixed Tissue Analysis. *J Vis Exp, 148,* 59633
8. Lee, S. J., Lee, C. K., Kang, S., Park, I., Kim, Y. H., Kim, S. K., Hong, S. P., Bae, H., He, Y., Kubota, Y. & Koh, G. Y. (2018) Angiopoietin-2 exacerbates cardiac hypoxia and inflammation after myocardial infarction. *J Clin Invest 128*, 5018-5033
9. Moritz, F., Schniering, J., Distler, J. H. W., Gay, R. E., Gay, S., Distler, O. & Maurer, B. (2017) Tie2 as a novel key factor of microangiopathy in systemic sclerosis. *Arthritis Res Ther 19*, 105
10. Vadivel, A., Alphonse, R. S., Etches, N., van Haaften, T., Collins, J. J., O'Reilly, M., Eaton, F. & Thébaud, B. (2014) Hypoxia-inducible factors promote alveolar development and regeneration. *Am J Respir Cell Mol Biol 50*, 96-105
11. Li, G., Sachdev, U., Peters, K., Liang, X. & Lotze, M. T. (2019) The VE-PTP Inhibitor AKB-9778 Improves Antitumor Activity and Diminishes the Toxicity of Interleukin 2 (IL-2) Administration. *J Immunother 42*, 237-243
12. Chan, W. W., Wise, S. C., Kaufman, M. D., Ahn, Y. M., Ensinger, C. L., Haack, T., Hood, M. M., Jones, J., Lord, J. W., Lu, W. P., Miller, D., Patt, W. C., Smith, B. D., Petillo, P. A., Rutkoski, T. J., Telikepalli, H., Vogeti, L., Yao, T., Chun, L., Clark, R., Evangelista, P., Gavrilescu, L. C., Lazarides, K., Zaleskas, V. M., Stewart, L. J., Van Etten, R. A. & Flynn, D. L. (2011) Conformational control inhibition of the BCR-ABL1 tyrosine kinase, including the gatekeeper T315I mutant, by the switch-control inhibitor DCC-2036. *Cancer Cell 19*, 556-568
13. Pittet, M. J., Garris, C. S., Arlauckas, S. P. & Weissleder, R. (2018) Recording the wild lives of immune cells. *Sci Immunol 3*, 1-12
14. Kim, E., Yang, K. S., Kohler, R. H., Dubach, J. M., Mikula, H. & Weissleder, R. (2015) Optimized Near-IR Fluorescent Agents for in Vivo Imaging of Btk Expression. *Bioconjug Chem 26*, 1513-1518

15. Lukinavičius, G., Blaukopf, C., Pershagen, E., Schena, A., Reymond, L., Derivery, E., Gonzalez-Gaitan, M., D'Este, E., Hell, S. W., Wolfram Gerlich, D. & Johnsson, K. (2015) SiR-Hoechst is a far-red DNA stain for live-cell nanoscopy. *Nat Commun 6*, 8497
16. Lukinavičius, G., Reymond, L., Umezawa, K., Sallin, O., D'Este, E., Göttfert, F., Ta, H., Hell, S. W., Urano, Y. & Johnsson, K. (2016) Fluorogenic Probes for Multicolor Imaging in Living Cells. *J Am Chem Soc 138*, 9365-9368
17. Meimetis, L. G., Giedt, R. J., Mikula, H., Carlson, J. C., Kohler, R. H., Pirovich, D. B. & Weissleder, R. (2016) Fluorescent vinblastine probes for live cell imaging. *Chem Commun (Camb) 52*, 9953-9956
18. Miller, M. A., Kim, E., Cuccarese, M. F., Plotkin, A. L., Prytyskach, M., Kohler, R. H., Pittet, M. J. & Weissleder, R. (2017) Near infrared imaging of Mer tyrosine kinase (MERTK) using MERi-SiR reveals tumor associated macrophage uptake in metastatic disease. *Chem Commun (Camb) 54*, 42-45
19. Dalton, A. C., Shlamkovitch, T., Papo, N. & Barton, W. A. (2016) Constitutive Association of Tie1 and Tie2 with Endothelial Integrins is Functionally Modulated by Angiopoietin-1 and Fibronectin. *PLoS One 11*, e0163732
20. Sturk, C. & Dumont, D. J. (2010) Tyrosine phosphorylation of Grb14 by Tie2. *Cell Commun Signal 8*, 30
21. Lukinavičius, G., Umezawa, K., Olivier, N., Honigmann, A., Yang, G., Plass, T., Mueller, V., Reymond, L., Corrêa, I. R., Luo, Z. G., Schultz, C., Lemke, E. A., Heppenstall, P., Eggeling, C., Manley, S. & Johnsson, K. (2013) A near-infrared fluorophore for live-cell super-resolution microscopy of cellular proteins. *Nat Chem 5*, 132-139
22. Motoike, T., Loughna, S., Perens, E., Roman, B. L., Liao, W., Chau, T. C., Richardson, C. D., Kawate, T., Kuno, J., Weinstein, B. M., Stainier, D. Y. & Sato, T. N. (2000) Universal GFP reporter for the study of vascular development. *Genesis 28*, 75-81
23. Mikula, H., Stapleton, S., Kohler, R. H., Vinegoni, C. & Weissleder, R. (2017) Design and Development of Fluorescent Vemurafenib Analogs for In Vivo Imaging. *Theranostics 7*, 1257-1265

Figures

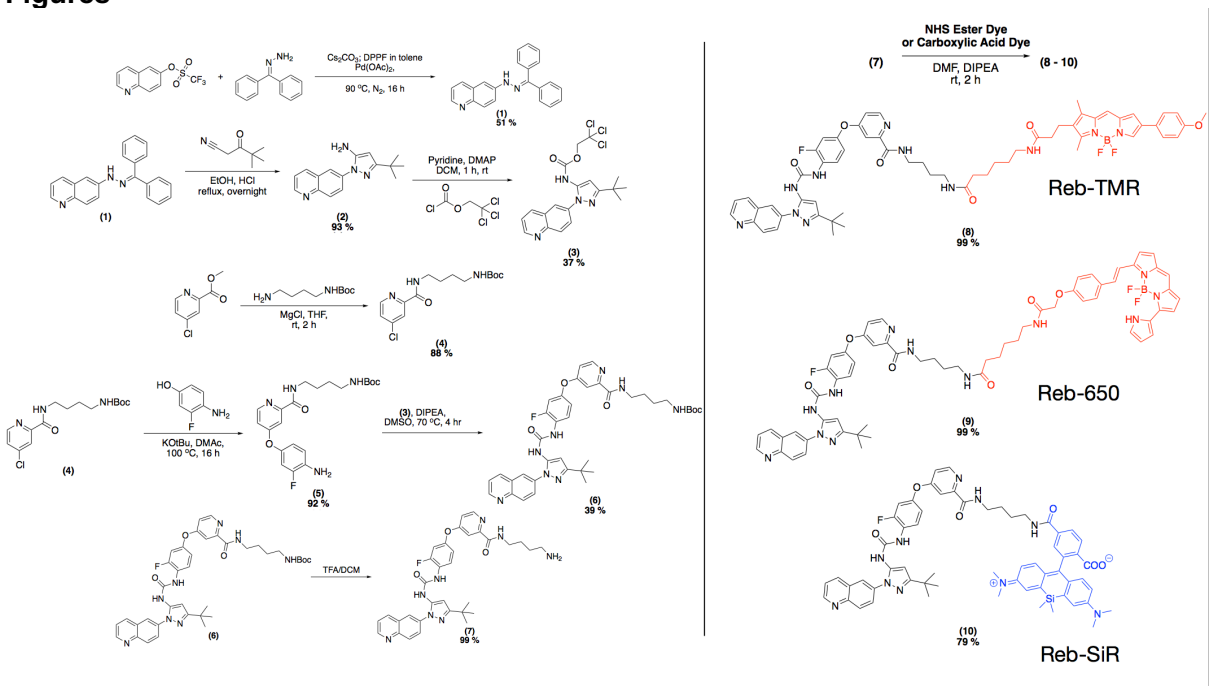

Figure 1: Synthesis of fluorescently labeled rebastinib derivatives. The synthesis of labeled rebastinib was completed using the scheme depicted above.

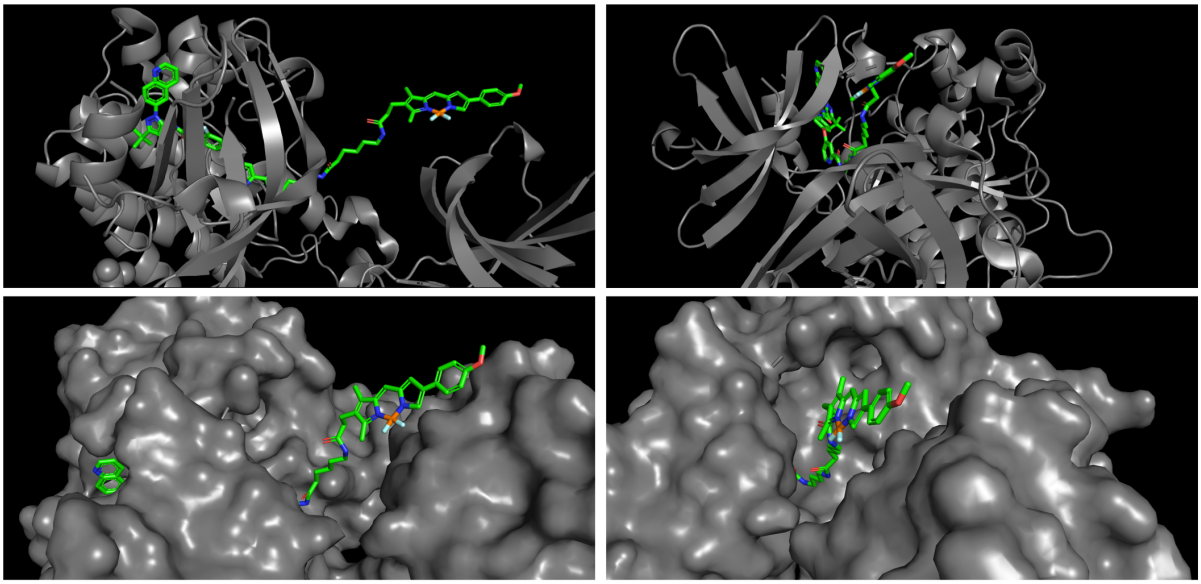

Figure 2: Modeling. Addition of a linker to the amide of rebastinib allows for coupling of a fluorophore to the small molecule. Based on a previously published structure of rebastinib in complex with Tie2 (PDB: 6MWE), we predicted this addition should not interfere with binding of rebastinib to Tie2.

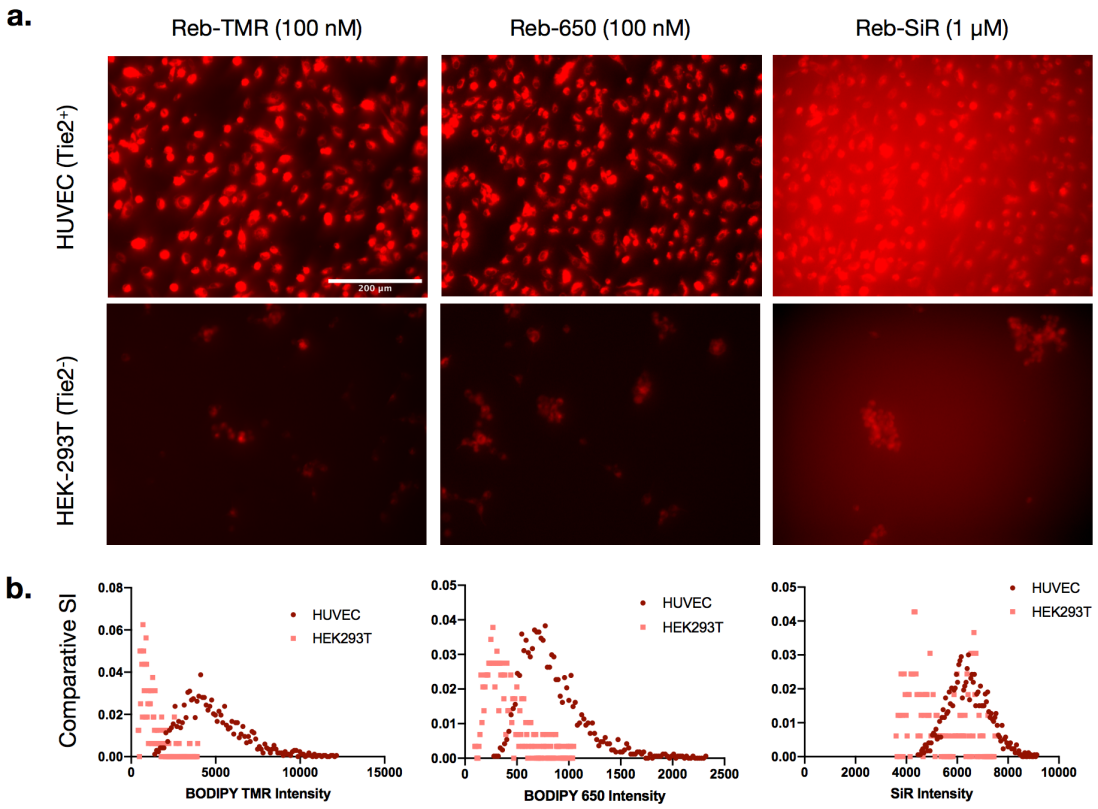

Figure 3: *In vitro* testing. Staining of HUVEC and HEK293T cells with the three fluorescent analogs of rebastinib. (a). Panel of representative images of Reb-TMR (100 nM), Reb-650 (100 nM), and Reb-SiR (1 uM) in HUVEC (Tie2+) and HEK293T (Tie2-) cell lines. Reb-TMR and Reb-650 stain HUVEC cells strongly, whereas the Reb-SiR analog stains cells weakly. (b) Quantification of fluorescent intensities in HUVEC and HEK293 cells at single cell resolution. Reb-TMR shows the strongest differential between HUVEC and HEK293T cells.

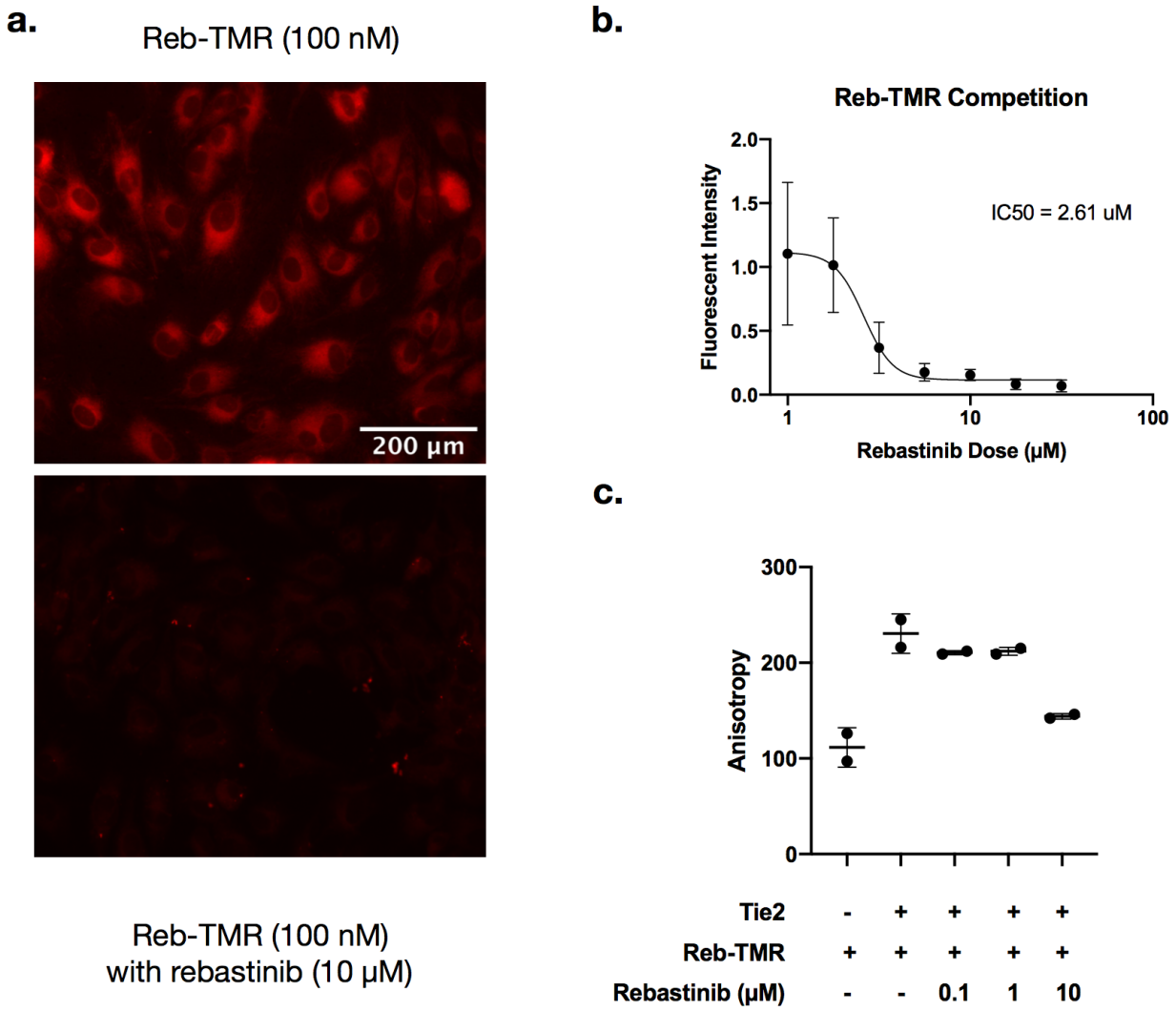

Figure 4: Quantitative binding data and inhibition of Reb-TMR (a) Representative images of Reb-TMR in HUVEC cells in the presence (below) or absence (top) of unlabeled rebastinib (10 uM). (b) Quantification of Reb-TMR fluorescent intensity as a function of increasing concentration of unlabeled rebastinib. Reported is the mean single cell fluorescent intensity per well, N = 2 wells. Error bars correspond to S.D. (c) Biochemical fluorescent polarization assay of rebastinib-bodipy TMR (0.8 uM) on enzymatic domain of Tie2. Leftmost point corresponds to polarization of Reb-TMR in PBS, and right points correspond to polarization of Reb-TMR with Tie2, and in increasing concentrations of unlabeled rebastinib (0,0.1,1,10 uM). Reported is mean over N = 2 wells. Error bars correspond to S.D.

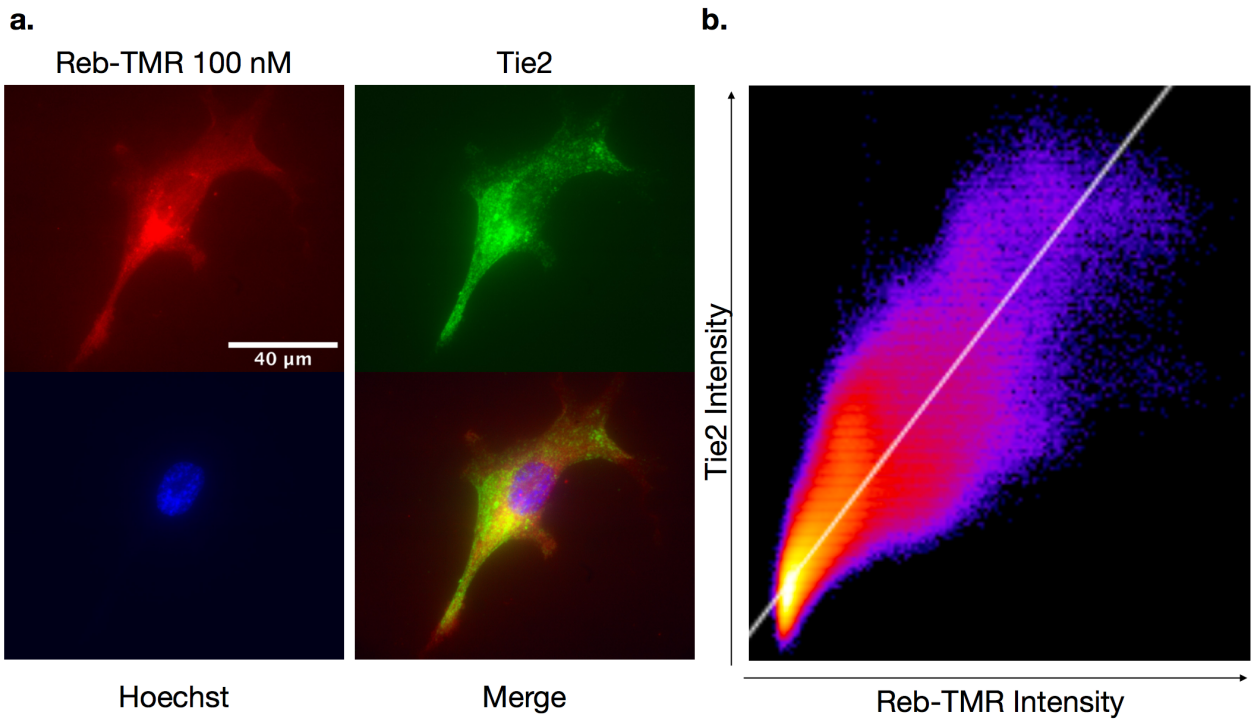

Figure 5: Co-localization (a) High resolution imaging of HUVECs. Treatment of HUVECs with Reb-TMR (100 nM) followed by a stain for Tie2 shows colocalization of the two markers in the cytoplasm (b) Correlation of Reb-TMR and Tie2 immunofluorescence signals (Pearson r^2 = 0.88)

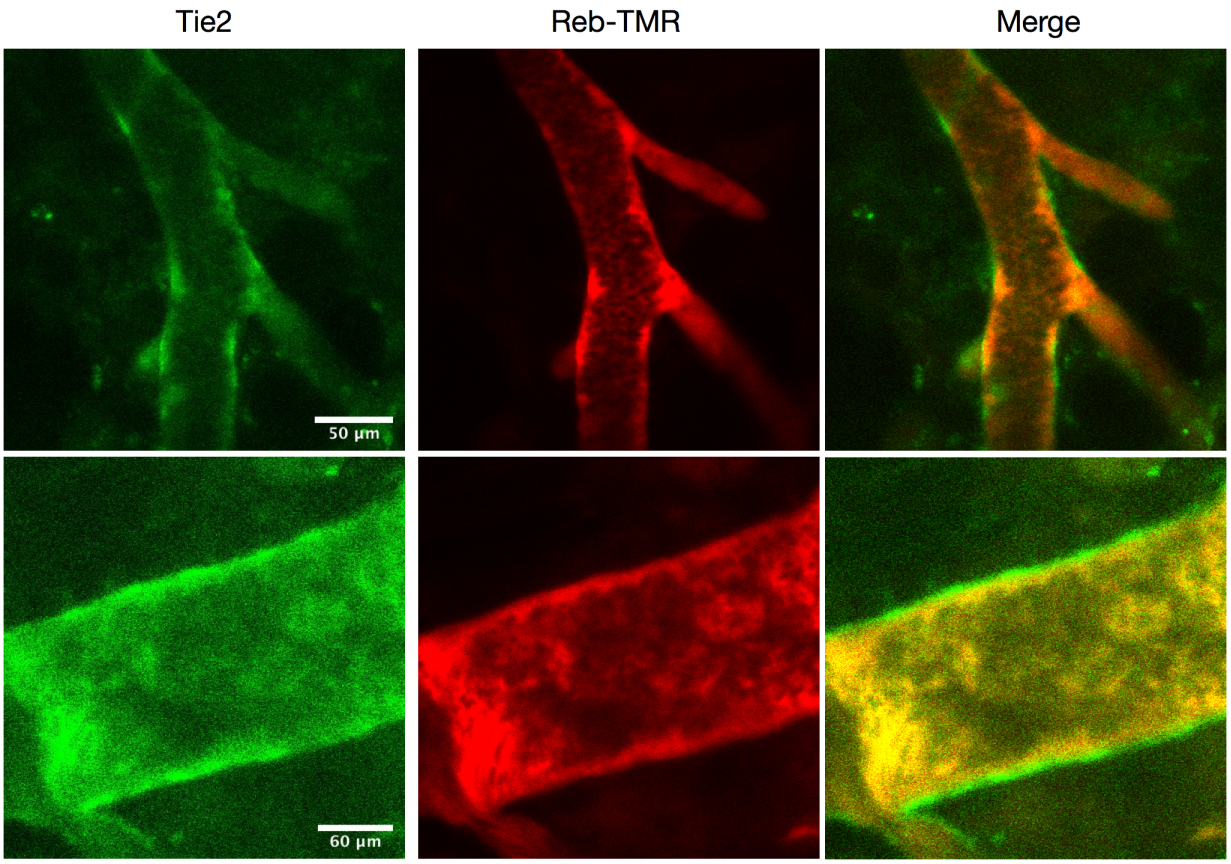

Figure 6: Intravital Microscopy. Tie2 reporter mouse, with implanted dorsal skin chambers, were injected with Reb-TMR (20 mg/kg, tail vein I.V.). About 1 hour after injection, select sites in the vascularized region were imaged. The two sites above show Reb-TMR lining the endothelia of the blood vessels, overlaying Tie2.

Table of Contents Graphic